Scan Outlier Ratio (ScOR): LiDAR Scanning and Survey-Aware Filtering of Detached Points in Terrestrial and Permanent Laser Scanning Point Clouds

Ronald Tabernig[1,2], Bernhard Höfle[1,2]

[1] 3DGeo Research Group, Institute of Geography, Heidelberg University, Germany– (ronald.tabernig, hoefle)@uni-heidelberg.de
[2] Interdisciplinary Center for Scientific Computing (IWR), Heidelberg University, Germany

Keywords: 3D Change Analysis, Outlier Removal, Terrestrial Laser Scanning, Permanent Laser Scanning.

ABSTRACT

Accurate 3D surface reconstruction and change analysis relies on point clouds representing persistent solid surfaces and should neglect very small (< laser footprint size) and temporary objects that create outliers. Terrestrial and Permanent Laser Scanning (TLS/PLS) data often contains transient or detached points, which violate assumptions of common cloud-, mesh-, and surface-based 3D change analysis methods. Those points cause wrong correspondences and affect change values in multi-temporal point cloud comparison. We address this with the Scan Outlier Ratio (ScOR) filter, a LiDAR scanning and survey-aware descriptor designed to identify points unsuitable for most point cloud-based change analysis methods. ScOR compares the measured point spacing with the expected spacing, assuming the surface is locally planar and orthogonal to the incoming laser beam. ScOR works with a single scan or multiple scans acquired from the same position, enabling multi-temporal neighborhoods for filtering. Using data from natural and urban environments, we analyze ScOR across different surfaces, neighborhood sizes, temporal neighborhoods, and compare it with the Statistical Outlier Removal (SOR) algorithm. Results show that ScOR successfully removes non-surface points, while preserving surface information. In our experiments, the true positive rate exceeds 95% in all but one case, while the false positive remains below 10% throughout. With neighborhoods from subsequent and aggregated epochs, the method automatically detects and removes large temporary objects (e.g., a person). Due to its interpretability, efficiency, and range-aware design, ScOR provides an effective pre-processing method for automated and near real-time 3D surface change analysis with TLS/PLS.

1. Introduction

Terrestrial Laser Scanning (TLS) allows capturing highly detailed point clouds (e.g., sub-centimeter point spacing and accuracy) and has been widely applied for monitoring tasks of the built and natural environment (Eitel et al., 2016). Permanently installed TLS systems (PLS) extend this capability to mostly autonomous and automatic monitoring from a fixed scan position with high temporal resolution (even sub-hourly) (Lindenbergh et al., 2025). Recently, ad hoc PLS systems used for environmental monitoring even enable super high temporal resolution of nearly continuous scanning and scan repetitions below 1 min (Meyer et al., 2025). Both multi-temporal TLS and PLS capture point clouds that are used for detecting and quantifying surface change over time (Kharroubi et al., 2022).

Most 3D change-analysis methods working on point cloud pairs go beyond nearest-neighbor distances and explicitly consider local point neighborhoods to establish correspondences across epochs (Yang and Holst, 2025). For example, M3C2 estimates per-point distances by fitting a local plane within a spherical neighborhood whose radius (i.e., “scale”) can be determined automatically to maximize planarity (Lague et al., 2013). Across methods, the main critical design choice is how these local neighborhoods and surface representations (e.g., local plane) are defined by the used method in order to establish correspondences (Yang and Holst, 2025). Consequently, inputs that do not form coherent, surface-like representations violate the underlying assumptions of these change analysis methods and result in wrong correspondences. Such inputs may result from small vegetation parts, insects, rain drops, ghost points at edges, or larger moving objects existing only in one epoch (Kharroubi et al., 2022). Points from such objects are unsuitable for 3D surface change analysis and must be removed before applying the algorithm. This ensures that change is only determined between persistent surfaces that enable useful multi-temporal correspondences. This is especially relevant for natural hazards monitoring, where it is critical to detect all relevant changes while minimizing false alarms. Due to the large number of point clouds in PLS settings and the requirement for near real-time processing, manual outlier removal is impractical or even impossible. Therefore, outlier handling must be automated to ensure consistent and timely processing across epochs and to enable fully automated workflows (Tabernig et al., 2025a).

We define ‘outliers’ from the perspective of 3D surface change analysis. Consequently, outliers are non-surface points that are detached from their surroundings and not suitable as input for 3D surface change analysis. They violate local surface constraints of the algorithms. Furthermore, they will often not be existing or represented similarly across multiple point cloud epochs. Unlike points on consistent surfaces, they do not form persistent, connected neighborhoods. These outlier points hinder the detection of reliable correspondences between scans. After removing a part of the points using radiometric filters (Riegl, 2019), further outlier removal of TLS and PLS data is commonly performed with the Statistical Outlier Removal (SOR) algorithm (Rusu et al., 2008; Kromer et al., 2017; Winiwarter et al., 2022). However, SOR requires to set a global threshold that tends to remove more points at a greater scanning range due to the increased point spacing, limiting its effectiveness for strongly range-dependent point spacings that are common for TLS and PLS data. As a solution, we present the Scan Outlier Ratio (ScOR) filter for outlier detection. ScOR is a LiDAR scanning- and survey-aware metric for TLS and PLS point clouds that evaluates neighborhood consistency in both the scanner’s angular domain (horizontal and vertical angles) and the 3D object space. ScOR provides a direct measure of local surface coherence that

This contribution has been peer-reviewed. The double-blind peer-review was conducted on the basis of the full paper.
https://doi.org/10.5194/isprs-annals-XI-2-2026-155-2026

is inherently range-aware and easy to interpret. Points on continuous surfaces have values near 1.0, whereas detached or transient points approach low values close to 0.0. Through this design and the inclusion of multi-temporal neighborhoods, ScOR additionally and effectively differentiates stable surfaces from isolated or temporary objects, enabling automated, survey-aware filtering prior to 3D change analysis.

The main contributions of this paper are:

- introduction of ScOR as a novel metric for automatic outlier removal;
- analysis of ScOR behavior across different local neighborhood sizes and object/surface types;
- assessment of multi-temporal neighborhood capabilities;
- comparison with baseline point cloud filter (i.e., SOR) to evaluate the robustness and interpretability of ScOR as an operational outlier remover for 3D surface change workflows.

2. State of the art

Point cloud outlier removal is commonly performed with fixed-scale neighborhood filters (e.g., fixed radius, fixed number of neighbors, fixed octree depth) and thus often global settings. The majority of methods is working in the 3D Cartesian space (XYZ and attributes) and does not integrate information on survey and scanning properties. Methods mainly differ in how they define and evaluate local neighborhoods (Park et al., 2020; Szutor and Zichar, 2023). The Radius Outlier Removal (ROR) removes points that have fewer than a minimum number of neighbors within a fixed search radius. Performance depends on the chosen radius and neighbor threshold (Park et al., 2020). In TLS and PLS data, where Euclidean distance and thus point spacing increases with range, fixed radii (i.e., distance thresholds) introduce a range-dependent effect that results in an increased removal of points at greater distances. Octree-based variants use a fixed octree depth with the goal to improve memory and runtime efficiency, but they share the same fixed-scale limitation (Szutor and Zichar, 2023). The Local Outlier Factor (LOF) also assigns each point an outlier score based on relative neighborhood density by using a fixed search radius and is sensitive to density variations (Breunig et al., 2000). The Statistical Outlier Removal (SOR) algorithm computes, for each point, the mean distance to its k- nearest neighbors and removes points whose mean distance is unusually large relative to the global distribution (controlled by k and a standard deviation multiplier) (Rusu et al., 2008). Because thresholds are computed based on the overall point cloud spacing, effectiveness depends on the assumption of homogenous point spacing. SOR is available in CloudCompare (Girardeau-Montaut, 2025) and is widely used to remove outliers in TLS and PLS change analysis studies (Kromer et al., 2017; Winiwarter et al., 2022). Further approaches use Delaunay triangulations or occupancy grids to remove non-surface points (Kang et al., 2014; Schauer and Nüchter, 2018). In automotive applications, a key task is the removal of snow, rain, and transient objects (Heinzler et al., 2019; Park et al., 2020). Both range image and point cloud-based strategies have been developed for these tasks, often using additional cues such as signal intensity, echo width or the number of returns. However, these methods do not account for local surface assumptions and are not designed for pre-filtering for 3D surface-change analysis. The Echo Ratio (ER) is the method that is the most similar to ScOR. ER measures local transparency/roughness as the ratio of returns in a search sphere to those in a vertical cylinder of the same radius (Höfle et al., 2009). Like ScOR, it compares 2D and 3D neighborhoods and is highly useful for airborne and UAV laser scanning data, for which it was developed. It differs by using a fixed search distance, a vertical search cylinder, and a ratio of point counts per neighborhood, which makes it less suitable for TLS/PLS datasets.

3. Methods

Our method builds on the theoretical consideration that points on continuous terrain surfaces tend to form locally consistent neighborhoods in the scanning grid, whereas outliers do not. Accordingly, we define the Scan Outlier Ratio (ScOR) to quantify local consistency relative to an idealized surface (Fig. 1). In this study, we assume a local plane surface perpendicular to the beam direction as our reference surface, which is a suitable choice for point cloud-based change algorithms relying on local surface and normal estimates, such as M3C2, and also registration methods, such as ICP.

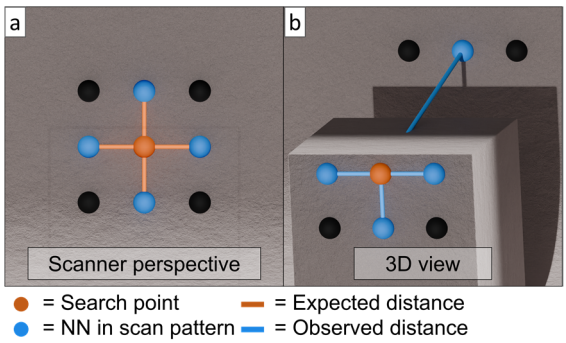

Figure 1. Side-by-side comparison of the expected 3D distance (orange line) from the scanner perspective (a) and the observed 3D distance (blue line) in object space (b). NN = nearest neighbor in scan angle domain.

3.1 Scan Outlier Ratio (ScOR) definition

The standard version of ScOR describes to what degree, between 0.0 (low) to 1.0 (high) a captured point cloud locally corresponds to the one that would be captured (i.e., expected point cloud) with the same scan settings on an idealized locally planar orthogonal surface at the respective distance. We further assume that the local surface exceeds the LiDAR footprint size (i.e., extended target) and the local point spacing by a multiple. To compute it, we assume a regular angular scan grid, i.e., laser measurements acquired with equal angular step widths in horizontal (φ) and vertical scan angle (θ). The standard version of ScOR assumes equal angular step widths and an orthogonal plane as the reference surface, but it can be adapted for use with different scan patterns and reference surfaces. For each point, we compute its angular position (φ, θ) relative to the scanner. Dividing these angles by the known scan resolutions ($\Delta\varphi$, $\Delta\theta$) and rounding to the nearest integers gives discrete grid indices that identify the corresponding row and column in the scan pattern. Neighborhoods are then defined in this scan grid. In the simplest case, we use the four immediate neighbors. One step above and below in θ (with fixed φ) and one step left and right in φ (with fixed θ). Larger neighborhoods can be obtained by increasing the offset (e.g., ±2 instead of ±1), which considers a broader surrounding at the cost of spatial detail. Due to our focus on terrain surfaces, we restrict neighborhood construction around last and single-return points. In vegetation or other complex environments, intermediate returns may belong to canopy layers or transient structures and would disturb neighborhood consistency (Jaboyedoff et al., 2012; Heinzler et al., 2019). For an ideal surface perpendicular to the incoming beam at the point of interest, the expected neighbor spacing in object space (i.e.,

3D Euclidean distance) arises from the given scan geometry. Specifically, for a point with range r and a chosen neighborhood offset k, the expected 3D distance d_{exp} to each of the four neighbors (as defined in Fig. 1) is

$$d_{exp} = r \cdot \tan(k \cdot \Delta\alpha), \quad (1)$$

where Δα is the angular scan resolution. We compare the expected distance with the measurements by retrieving each neighbor’s coordinates and computing its 3D Euclidean distance to the central point (Fig. 1). The mean values of the observed distances $\bar{d}_{obs}$ and the mean of expected distances $\bar{d}_{exp}$ are then computed and compared, providing an empirical measure of neighborhood consistency in object space. We then define the Scan Outlier Ratio for a point as

$$\text{ScOR} = \min\left(1, \frac{\bar{d}_{exp}}{\bar{d}_{obs}}\right), \quad (2)$$

where $\bar{d}_{obs}$ is the mean of the observed distances and $\bar{d}_{exp}$ is the mean of expected distances. ScOR values near 1.0 indicate locally consistent neighborhoods oriented orthogonally to the incident beam, whereas values near 0.0 highlight detached or isolated points (e.g., bees, birds, moving vegetation) that we classify as outliers. Values greater than 1.0 can occur due to deviations from an ideal grid caused by the non-deterministic nature of LiDAR sampling. When sampling at a fixed resolution, the actual grid is not perfectly uniform because of angular deviations and beam-target interaction effects. This leads to cases where expected distances exceed the observed ones, resulting in ScOR>1.0. Such areas are not the focus of further analysis, and all ScOR greater than 1.0 are set to 1.0 (Eq. 2).

Using an angular discretization equal to the scanner’s native sampling can introduce aliasing that becomes apparent in subsequent processing stages. To prevent aliasing, we oversample the angular grid following the Nyquist–Shannon sampling criterion (Nyquist, 1928; Shannon, 1949), ensuring that the discretization exceeds twice the scanner’s angular resolution. In practice, we multiply the scan resolution by two and add a small value corresponding to the angular accuracy of the measuring device. This satisfies the sampling criterion and provides a conservative safety margin. All subsequent computations are performed using the oversampled angular grid to index the discrete cells.

3.2 Experiments on surface-specific ScOR behavior

To investigate the changes of ScOR across different surface types and geometries, we present the spatial distribution of ScOR and corresponding histograms for each case. For this purpose, we use PLS data of (a) a rockfall study site (Czerwonka-Schröder et al., 2025) and (b) an urban environment. We apply a reflectance filter to remove points with very low (<-25 dB) or excessively high reflectance values (>5 dB), which often correspond to dust, haze, or artificial targets (Riegl, 2019; Wittke et al., 2024). We use the radiometric filter because our method is designed to work alongside reflectance-based filters, rather than replacing them. For the rockfall study site, we analyze a subset of the time series comprising 24 hours of hourly measurements (24 epochs). For the urban area, we use a time series spanning 48 minutes, with data collected every two minutes (24 epochs). At the rockfall site, we focus on two specific areas. The first is a small patch of the outcrop containing holes, edges, and rock faces with different orientations (Fig. 2a). This patch is of particular interest because it includes all critical surface types commonly analyzed in rockfall studies, allowing us to examine how ScOR behaves in these areas. The second area consists of a tree, which is of interest because it consists of thick trunks and branches of different sizes, and a lot of leaves (Fig. 2b). Here, we want to assess how these differences in structure and size are represented by ScOR and, accordingly, if we are able to remove the small vegetation parts.

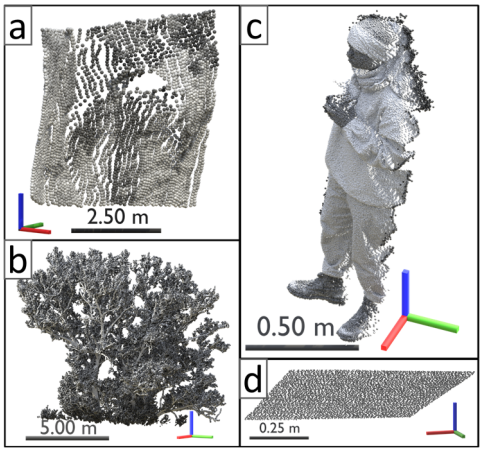

Figure 2. The four areas used to investigate ScOR behavior. The selected areas include the rock outcrop (a), a tree (b), a person (c), and a paved floor (d). The first column shows each area from the rock outcrop dataset, while the second column shows each area from the urban dataset. Colored by intensity.

In the urban environment, we focus on two patches. One contains a person (Fig. 2c) and another consists of a paved ground (Fig. 2d). The patch containing the person is selected for two reasons. Firstly, it exhibits numerous point cloud ghosting effects at edges and isolated points. Secondly, while the person itself represents a stable surface within a single epoch, it also represents a temporary object in the overall time series. This makes this patch especially interesting for studying how ScOR can be used in cases of temporary occlusions and for the removal of large dynamic objects that are not present in every epoch. Another interesting element is the paved ground, considering that ScOR is designed to produce the highest values for planar surfaces oriented orthogonally to the scanner. Although the paved surface is mostly planar, its orientation deviates substantially from this ideal configuration. Nevertheless, planes with incidence angles smaller than 90° often occur in areas relevant for surface change analysis, since TLS often involves looking at slanted angles to ground surfaces. Considering this, we select the paved ground as the second patch in the urban area to illustrate ScOR behavior at small incidence angles. To investigate the impact of neighborhood size on ScOR, we vary the angular step widths. Using the same areas as before, we compute ScOR with neighborhoods constructed using step widths two to three times larger than the baseline. This allows us to assess whether larger neighborhoods detect outlier clusters that appear to be locally connected at spatially detailed scales.

3.3 Multi-temporal neighborhoods for PLS setups

So far, ScOR has been introduced for computation within a single epoch. For point cloud time series where all epochs are acquired from the same scan position, as is typically the case in PLS, surfaces observed across multiple epochs can provide information that is not accessible in single-epoch analyses, including the detection of large moving objects that cause temporary occlusions (Schachtschneider et al., 2017). In standard ScOR application, points from a single epoch are used as search points and as neighbor candidates. We extend the method to allow the use of multi-temporal neighborhoods. In this

configuration, one epoch is defined as the reference epoch for which ScOR is computed. With multi-temporal neighborhoods, the points considered for neighborhood construction are then replaced by points acquired from other epochs (Fig. 3). For each point of the reference epoch, ScOR is then computed using a neighborhood derived from another epoch. We further distinguish two approaches for multi-temporal neighborhoods.

The first approach uses a single epoch that differs from the reference epoch used for the search points. The selected epoch may precede or follow the reference epoch in time, and the time passed between the two epochs is freely defined. This approach is sensitive to temporal differences between the selected epoch and the reference epoch. To examine this effect, we compute a time series where the reference epoch is fixed and ScOR is evaluated using multi-temporal neighborhoods for each epoch of the time series, including the search epoch (standard configuration). This allows us to investigate whether the neighborhood characteristics of surface patches of the reference epoch vary over time.

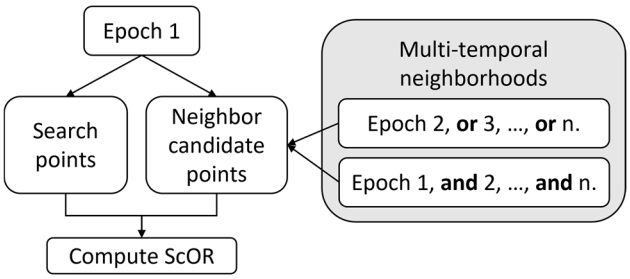

Figure 3. Illustration of the standard ScOR computation and its extension using multi-temporal neighborhoods. The example shows epoch 1 as the reference, but the temporal order of the epochs used for search points and the number of aggregated epochs can be chosen freely. Multi-temporal neighborhoods separated by “or” indicate that points are taken from a single other epoch as neighborhood candidates, whereas “and” indicates two or more freely selectable epochs that are aggregated and used as neighborhood candidates.

The second approach employs multi-temporal neighborhoods composed of two or more temporally aggregated epochs, which may or may not include the reference epoch (Tabernig et al., 2025b). The number of aggregated epochs and the inclusion of the reference epoch in neighborhood queries are freely adjustable parameters. This approach is expected to be less sensitive to temporal variations between individual epochs and likely to introduce an averaging effect by assigning an equal weight to all aggregated epochs. In this study, we focus on temporally aggregated neighborhoods that include the search epoch. For this purpose, we compute nine different levels of aggregation (LoA) ranging from one to nine, where LoA defines the number of epochs merged into a single point cloud (Tabernig et al., 2025b). LoA 1 in this case is the non-aggregated standard configuration.

3.4 Range-dependent filtering of detached point clusters

Given that our goal is to demonstrate the capability of ScOR for outlier removal at single scan positions, we compare it to the Statistical Outlier Removal (SOR) method. We consider both overall performance and range dependent performance, where performance is measured as the potential to detect outliers while retaining surface points. For the specific case of detached or floating points from single scan positions, we use a manually annotated single scan position point cloud acquired in an alpine environment. This point cloud is used as an example of a challenging dataset. Even after radiometric filtering, it contains many detached floating points and clusters at ranges up to 45 m. Each point is labeled as outlier or inlier: True positives (TP) are correctly detected outliers, false positives (FP) are surface points incorrectly detected as outliers, false negatives (FN) are outliers not detected, and true negatives (TN) are surface points correctly retained. To assess performance at different ranges of SOR and ScOR, we group points into 5 m bins from 0 to 45 m, covering the region containing outliers. For SOR, we vary the number of neighbors $k \in \{3,6,12,24,48,96\}$ and the standard deviation multiplier $\in \{0.5,1.0,1.5,2.0,2.5\}$. ScOR offers a continuous threshold between 0.0 and 1.0. We move the threshold in small increments of 0.01, compute overall Youden’s J (TP Rate minus FP Rate) for each value, and select the threshold that maximizes Youden’s J. Points with a ScOR value below this threshold are classified as outliers. We then compare the outlier removal performance of each SOR parameter combination to the selected ScOR threshold across range bins, giving insights to the stability of ScOR across different distances and for comparison with SOR performance. For this, we show both the true positive rate (TPR) and the false positive rate (FPR) per range bin of all parameter combinations of SOR and for the determined threshold for the ScOR. To further investigate the point cloud differences, we select an SOR parameter combination that performs near the average in both TPR and FPR. This allows us to compare the types of points removed by ScOR and SOR. We choose an average-performing configuration because SOR parameters involve a strong trade-off between TPR and FNR. Hereby, we do not aim to identify the method that is better or worse overall. Using this configuration, we aim to enhance the understanding of which outliers are removed by each of the two methods, including isolated floating points, small clusters, and other detached points.

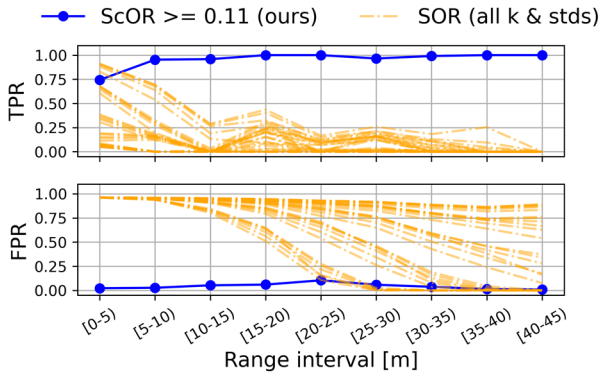

Figure 4. Comparison of true positive rate (TPR) and false positive rate (FPR) across different ranges for all SOR parameter combinations and for ScOR using a threshold of 0.11. Results are based on a single scan position acquired in an alpine environment containing numerous outliers.

4. Results

4.1 Range-dependent filtering of detached point clusters

Using Youden’s J, a ScOR threshold of 0.11 was determined to be suitable for removing floating and detached points. This threshold is applied in all subsequent analyses. As shown in Fig. 4, both the TPR and FPR of ScOR remain stable across distance ranges, with only a slight decrease in performance at close range. In contrast, no parameter combination for SOR achieves both a high TPR and a low FPR simultaneously. These findings are consistent with the spatial comparison in Fig. 5, where neither ScOR nor SOR fully remove all points located near

This contribution has been peer-reviewed. The double-blind peer-review was conducted on the basis of the full paper.
https://doi.org/10.5194/isprs-annals-XI-2-2026-155-2026 | © Author(s) 2026. CC BY 4.0 License.

the center. From this perspective, it becomes evident that at larger ranges, ScOR removes fewer non-outlier points than SOR, as also shown in Fig. 4. In Fig. 5 it only visually appears as if at close range SOR outperforms ScOR in terms of outlier removal. Closer visual inspection makes it apparent that SOR is primarily more effective at removing single isolated points, but cannot remove small, detached clusters. Such clusters commonly occur in the presence of insects or similar transient objects. This results in an overall lower performance of every parameter combination used for SOR compared to a single ScOR threshold, as shown in Fig. 4.

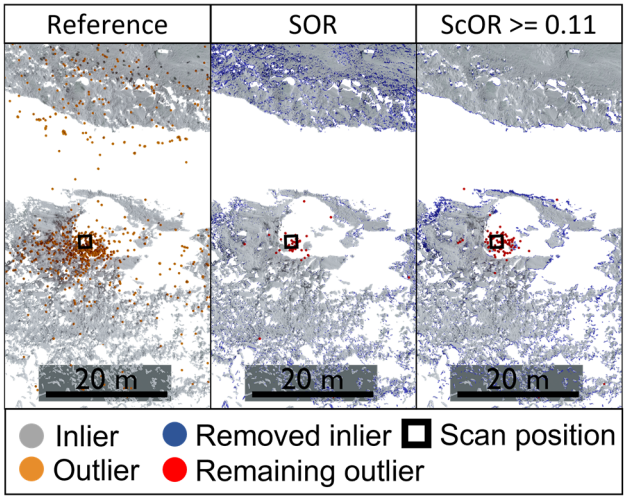

Figure 5. Spatial comparison of SOR and ScOR results using ScOR filtering with a threshold of 0.11 and SOR with k=12 and a standard deviation multiplier of 2.0. The selected SOR configuration represents a parameter set that performs well across different ranges. The shown area is from a single scan position acquired in an alpine environment containing numerous outliers.

4.2 Surface-specific ScOR behavior

The spatial distribution of ScOR across different surface types (Fig. 6) and the corresponding histograms (Fig. 7) confirm the expected theoretical behavior. We observe that (1) homogeneous surfaces such as paved floors exhibit highly uniform ScOR values, whereas complex surfaces such as a person or a rock outcrop show a broader value spread. (2) Small incidence angles, as seen for the paved floor, result in lower ScOR values. Still, the local neighborhoods remain sufficiently connected in the point cloud, which maintains ScOR values well above zero, i.e., between 0.2 and 0.4. (3) Edges and curved regions, such as those at the convex and concave areas in the rock outcrop and the outline of the person, display smaller ScOR values than their flat surroundings. (4) For the tree, which consists of a solid trunk and branches as well as more dynamic leaves and smaller branches, ScOR varies substantially. Linear structures with minimal breadth, including small branches and twigs, as well as small point clusters representing leaves, exhibit very low ScOR values (<0.11), whereas thicker trunks and branches whose points are more connected in the point cloud representation show higher values. Points with ScOR above the threshold (0.11) appear to primarily belong to well-connected surfaces. (5) Detached points are clearly distinguishable, as their ScOR values are near zero, as illustrated for the person in Fig. 6.

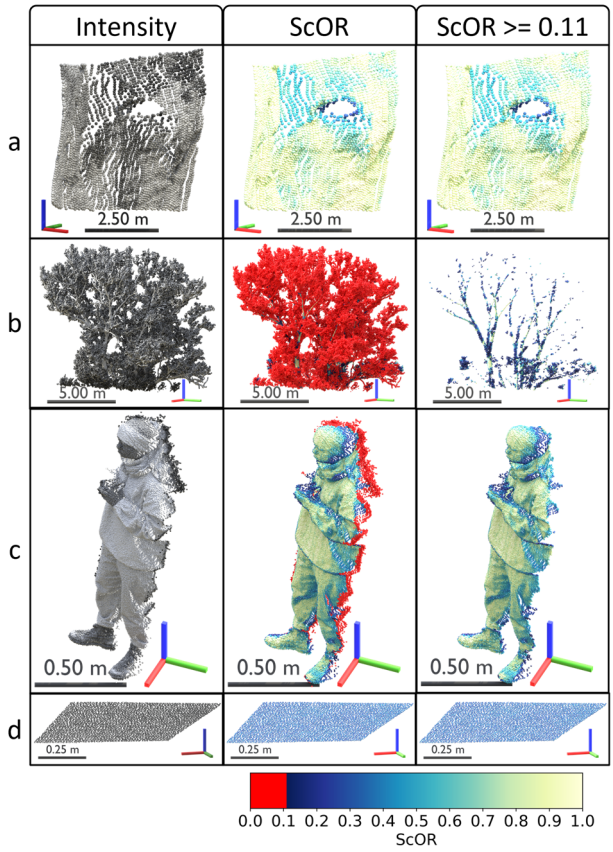

Figure 6. ScOR values in the four areas used to investigate ScOR behavior. The selected areas include the rock outcrop (a), a tree (b), a person (c), and a paved floor (d). The first column shows each area colored by intensity, while the second and third columns show the same areas colored by ScOR. Red points in the second column indicate ScOR values below 0.11 and are not displayed in the third column.

Overall, the rock outcrop and the person attain the highest ScOR values, followed by the paved floor, whereas the tree exhibits the lowest values, mostly just above zero due to the presence of leaves and other small components. Increasing the neighborhood size by two or three increments results in minor changes. The most relevant observation is that larger neighborhoods introduce spatial smoothing, which reduces the effect originating from small-scale local roughness. Although ScOR increases slightly with neighborhood size, the overall distribution remains largely unchanged.

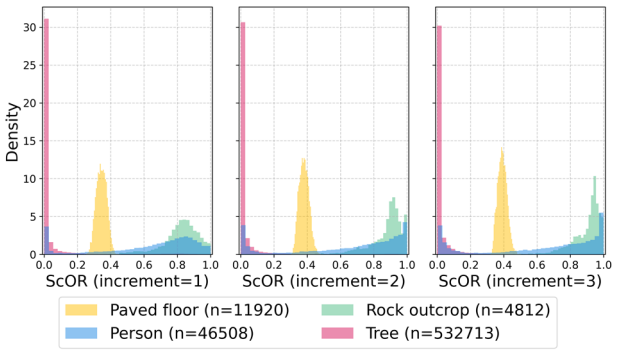

Figure 7. Histograms of ScOR values for each investigated surface type at increasing neighborhood sizes. Results show for neighborhood sizes at increment 1, 2, and 3.

This contribution has been peer-reviewed. The double-blind peer-review was conducted on the basis of the full paper.
https://doi.org/10.5194/isprs-annals-XI-2-2026-155-2026 | © Author(s) 2026. CC BY 4.0 License.

As the increment increases, existing trends become more distinct. This can be seen with the paved floor, the person, and the rock outcrop. Detached points near the person remain largely unaffected, maintaining their detectability across all neighborhood sizes. Bringing together insights produced so far, we present how removing points with low ScOR values affects the point cloud of the vineyard at the Trier study site (standard neighborhood size and ScOR>0.11) (Fig. 8). The main insights can be summarized in three aspects. (1) Branches and leaves of trees are largely removed, although some dense clusters remain. This provides a clearer view and point cloud of the rock outcrop, leaving mainly the slope, the rock outcrop, a few trunks, and dense vegetation clusters in this area. (2) The vine stocks are almost completely removed, with only a few points remaining at the location of their intersect with the ground. This results in a dataset composed primarily of ground points within the rockfall deposition area. (3) The overall number of points is reduced by 55.09% (5 771 565 points removed out of 10 477 434), while points relevant to the rock fall study site are retained. This implies that, at this stage, point clouds can already be substantially reduced, and with it the computational cost of subsequent processing steps.

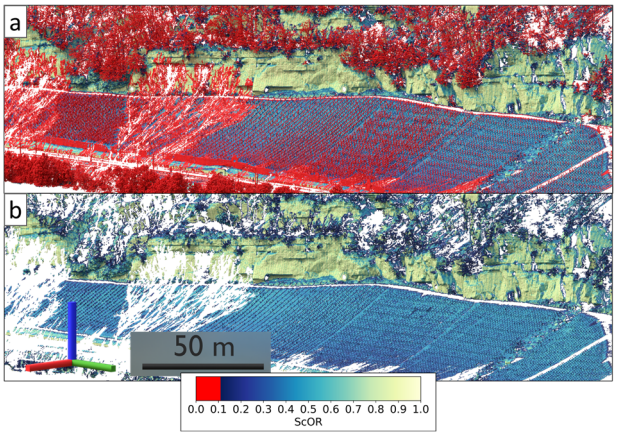

Figure 8. Comparison of Trier vineyard and rockfall outcrop before (a) and after (b) removing points with ScOR<=0.11. The dataset contains 10 477 434 points before filtering and 5 771 565 points after. Colored by ScOR.

4.3 Multi-temporal neighborhoods for PLS setups

As multi-temporal neighborhoods provide temporal context to identify transient objects, we consider the behavior of each selected area across its time series. In order to better understand object persistence, we compute ScOR using multi-temporal neighborhoods. The key observation is that the person’s ScOR immediately drops to zero when any other epoch is used for neighborhood construction (Fig. 9). This implies that the person was present only in a single epoch and demonstrates the possibility of using a neighborhood from a different epoch to identify and remove large temporary objects. For the rock outcrop, the tree, and the paved floor, no notable changes are observed. This indicates that the point cloud representation of these areas and their respective neighborhoods remains consistent across epochs. Given that increasing the Level of Aggregation (LoA) affects the point cloud representation, we examine its influence on ScOR for the selected surface types (Fig. 10). The person’s median ScOR drops to zero at LoA 2, where a multi-temporal neighborhood consisting of two epochs is used for neighborhood construction. For any larger LoA, the person’s ScOR remains consistently close to zero. This agrees with the results from time series analysis (Fig. 9), which indicates that the person was captured only in the first epoch, confirming it as a large moving object detectable with both single-epoch and aggregated epoch multi-temporal neighborhood approaches. For the rock outcrop, the tree, and the paved floor, increasing the LoA results in no distinguishable change in the median ScOR or in the 25th–75th percentile range. These observations suggest that both single-epoch and aggregated multi-epoch neighborhoods are suitable for identifying dynamic objects due to the strong variation in their neighborhood representations of the person across time.

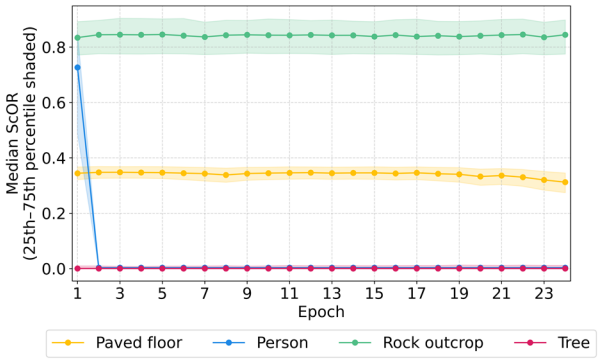

Figure 9. Time series of median ScOR values for each investigated surface type by using only single other epochs for multi-temporal neighborhoods construction. Shaded regions represent the 25th–75th percentile per surface type.

In order to better understand how ScOR responds to both small detached points and larger temporary structures, we distinguish three use cases: (1) the removal of detached points that do not belong to a consistent surface (Fig. 11b), (2) the removal of a well-represented but transient object using a single other epoch as the multi-temporal neighborhood (Fig. 11c), and (3) the removal of such an object using aggregated epochs for the neighborhood (Fig. 11d). For the first use case, removal of detached points, ghosting points are effectively eliminated using low ScOR thresholds (<0.11), demonstrating the sensitivity of the method to isolated, non-persistent points.

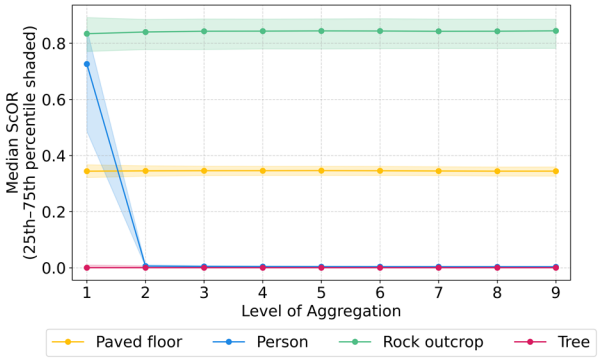

Figure 10. Variation in median ScOR values and the 25th–75th percentiles with increasing levels of aggregation (LoA) for each surface type.

When multi-temporal neighborhoods are used (second and third use case), the person is easily detected, as the local context changes from being dominated by points representing the person itself to being composed mainly of ground points that were occluded in the reference epoch. The comparison also shows slightly higher values in the area where the feet touch the ground, resulting from their spatial proximity to the persistent neighborhood. This effect is slightly amplified in the aggregated

multi-temporal neighborhood. The behavior arises from the neighborhood being constructed from both the reference and another epoch, illustrating the weighting of both epochs compared to considering only one other epoch. This demonstrates the ability to remove both small detached clusters and large transient objects that do not persist across epochs.

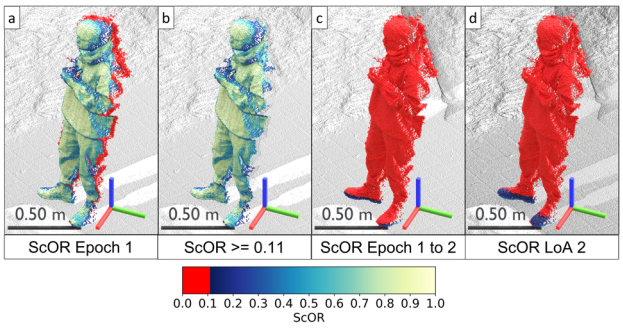

Figure 11. Comparison of (a) the distribution of ScOR values for the person, (b) the person after removing points with ScOR below 0.11, (c) ScOR values computed for points from epoch 1 using multi-temporal neighborhood with points from epoch 2, and (d) ScOR values computed for points from epoch 1 using multi-temporal neighborhood points from temporally aggregated epochs 1 and 2. Black points show surrounding points taken from either a single- or multi-temporal neighborhood.

5. Discussion

Three practical applications of ScOR can be identified. The first involves expert-based thresholding. Following the thresholds presented in this study, users may adjust the method according to their objectives. Although the threshold of 0.11 performed consistently well across three substantially different datasets, its applicability to other data should be verified before general use. The second application is automated threshold determination. ScOR can be computed for an entire scene, and histogram-based clustering can identify thresholds automatically. The third is interactive adjustment. Thresholds can be modified using e.g., the slider function in CloudCompare, providing an intuitive way to balance trade-offs between outlier removal and surface preservation. Once the threshold is determined, it can be used for entire point cloud time series of a PLS setup.

The comparison between SOR and ScOR shows that ScOR remains stable across varying ranges. Both methods address different purposes. SOR is sensitive to point spacing and therefore less suitable for single scan TLS data with points at close to very long range, while ScOR is more robust under such conditions. As a practical strategy, we suggest applying ScOR as a preliminary filter before merging multiple single scan TLS positions and applying SOR. Doing so, ScOR can be used with very small thresholds to remove clusters of detached points in point clouds with strongly varying point densities, allowing SOR to handle remaining isolated points in merged point clouds where multiple scan positions may contribute to a more equal distribution of point densities. This sequential approach combines their advantages and reduces the risk of removing valid surface points.

It is important to note that in this study, outliers are defined as points unsuitable for surface change analysis, which differs from the definition used in other frameworks (Park et al., 2020). The comparison therefore emphasizes that ScOR meets the specific requirements of surface change analysis. It must be considered that ScOR still shows moderate range dependence because larger neighborhoods are needed at greater distances to preserve local characteristics. For thin structures such as branches, the range dependence is particularly evident (i.e., changing relation between a constant object size and increasing point spacing), as fewer valid neighbors will be available at larger scan distances.

The use of multi-temporal neighborhoods proved effective for detecting and removing both small and large dynamic objects. Even one additional epoch improves filtering, though sensitivity to bi-temporal changes remains. Aggregating several epochs creates a more stable representation of neighborhoods that integrates all acquisitions and reduces the effects of short-term temporal fluctuations. The removal of detached points and small vegetation was demonstrated at the Trier study site. These results confirm that ScOR successfully extracts the ground surface and substantially reduces data volume by removing large parts of vegetation. This supports the main goal of the study, which is to prepare data for reliable 3D surface change analysis and to reduce processing requirements in subsequent steps.

6. Conclusion

We present ScOR (Scan Outlier Ratio), a TLS- and PLS-survey aware point cloud metric, designed as a filter for removing points unsuitable for 3D surface change analysis in point clouds. ScOR enables automatic reduction of point clouds to regions suitable for establishing surface correspondences throughout point cloud time series. This represents an important step before actual change computation that has so far mainly been performed manually. Our proposed method performs this step fully automatically on a point cloud-to-point cloud basis and further allows the use of multi-temporal neighborhoods. Future research should focus on assessing the influence of incorporating ScOR as a preprocessing step in established point cloud-based monitoring setups, thereby exploring potential improvements in computation time, the propagation and potential reduction of errors in downstream point cloud processing, segmentation and classification tasks. In addition, the use of multi-temporal neighborhoods within ScOR was shown to offer the possibility to extract small and large dynamic objects, either by isolating or by removing them. Therefore, the method can not only remove outliers, but also has the potential to remove background from dynamic scenes. In summary, ScOR provides a new strategy for preprocessing 3D point cloud time series with significant implications for informed data reduction and the detection of dynamic objects. The presented method will be released open-source (https://github.com/3dgeo-heidelberg) to facilitate its integration into existing 3D surface change analysis workflows.

Acknowledgements

This work is funded by the BMFTR AImon 5.0: Project no. 02WDG1696 and by the Deutsche Forschungsgemeinschaft (DFG, German Research Foundation) – no. 535733258 (Extract4D).

References

Breunig, M., Kröger, P., Ng, R., Sander, J., 2000. LOF: Identifying Density-Based Local Outliers. *ACM Sigmod Record*, 93-104. doi.org/10.1145/342009.335388

Czerwonka-Schröder, D., Schulte, F., Albert, W., Hosseini, K., Tabernig, R., Yang, Y., Höfle, B., Holst, C., Zimmermann, K., 2025. AImon5.0 - Real-time monitoring of gravitational mass movements for critical infrastructure risk management with AI-

assisted 3D metrology. In: *6th Joint International Symposium on Deformation Monitoring (JISDM)*. doi.org/10.5445/IR/1000179762

Eitel, J.U.H., Höfle, B., Vierling, L.A., Abellán, A., Asner, G.P., Deems, J.S., Glennie, C.L., Joerg, P.C., LeWinter, A.L., Magney, T.S., Mandlburger, G., Morton, D.C., Müller, J., Vierling, K.T., 2016. Beyond 3-D: The new spectrum of lidar applications for earth and ecological sciences. *Remote Sens. Environ.* 186, 372–392. doi.org/10.1016/j.rse.2016.08.018

Girardeau-Montaut, D., 2025. CloudCompare. Version 2.13.2. http://www.cloudcompare.org/ (29 October 2025).

Heinzler, R., Schindler, P., Seekircher, J., Ritter, W., Stork, W., 2019. Weather Influence and Classification with Automotive Lidar Sensors, In: *2019 IEEE Intelligent Vehicles Symposium*. 1527–1534. doi.org/10.1109/IVS.2019.8814205

Höfle, B., Mücke, W., Dutter, M., Rutzinger, M., Dorninger, P., 2009. Detection of building regions using airborne LiDAR : a new combination of raster and point cloud based GIS methods. In: *Geospatial Crossroads @ GI_Forum '09*. 66-75. doi.org/10.11588/heidok.00036990

Jaboyedoff, M., Oppikofer, T., Abellán, A., Derron, M.-H., Loye, A., Metzger, R., Pedrazzini, A., 2012. Use of LIDAR in landslide investigations: a review. *Nat. Hazards* 61, 5–28. doi.org/10.1007/s11069-010-9634-2

Kang, X., Liu, J., Lin, X., 2014. Streaming Progressive TIN Densification Filter for Airborne LiDAR Point Clouds Using Multi-Core Architectures. *Remote Sens.* 6, 7212–7232. doi.org/10.3390/rs6087212

Kharroubi, A., Poux, F., Ballouch, Z., Hajji, R., Billen, R., 2022. Three Dimensional Change Detection Using Point Clouds: A Review. *Geomatics* 2, 457–485. doi.org/10.3390/geomatics2040025

Kromer, R.A., Abellán, A., Hutchinson, D.J., Lato, M., Chanut, M.-A., Dubois, L., Jaboyedoff, M., 2017. Automated terrestrial laser scanning with near-real-time change detection – monitoring of the Séchilienne landslide. *Earth Surf. Dyn.* 5, 293–310. doi.org/10.5194/esurf-5-293-2017

Lague, D., Brodu, N., Leroux, J., 2013. Accurate 3D comparison of complex topography with terrestrial laser scanner: Application to the Rangitikei canyon (N-Z). *ISPRS J. Photogramm. Remote Sens.* 82, 10–26. doi.org/10.1016/j.isprsjprs.2013.04.009

Lindenbergh, R., Anders, K., Campos, M., Czerwonka-Schröder, D., Höfle, B., Kuschnerus, M., Puttonen, E., Prinz, R., Rutzinger, M., Voordendag, A., Vos, S., 2025. Permanent terrestrial laser scanning for near-continuous environmental observations: Systems, methods, challenges and applications. *ISPRS Open J. Photogramm. Remote Sens*. 17, 100094. doi.org/10.1016/j.ophoto.2025.100094

Meyer, J.S., Tabernig, R., Höfle, B., 2025. Detection of honey bees (Apis mellifera) in hypertemporal LiDAR point cloud time series to extract bee activity zones and times. *ISPRS Ann. Photogramm. Remote Sens. Spat. Inf. Sci. X-G-2025*, 583–590. doi.org/10.5194/isprs-annals-X-G-2025-583-2025

Nyquist, H., 1928. Certain Topics in Telegraph Transmission Theory. *Trans. Am. Inst. Electr. Eng.* 47, 617–644. doi.org/10.1109/T-AIEE.1928.5055024

Park, J.-I., Park, J., Kim, K.-S., 2020. Fast and Accurate Desnowing Algorithm for LiDAR Point Clouds. *IEEE Access* 8, 160202–160212. doi.org/10.1109/ACCESS.2020.3020266

RIEGL, 2019. Datasheet RIEGL VZ-2000i. RIEGL Laser Measurement Systems. Horn, Austria.

Rusu, R.B., Marton, Z.C., Blodow, N., Dolha, M., Beetz, M., 2008. Towards 3D Point cloud based object maps for household environments. *Robot. Auton. Syst.* 56, 927–941. doi.org/10.1016/j.robot.2008.08.005

Schachtschneider, J., Schlichting, A., Brenner, C., 2017. ASSESSING TEMPORAL BEHAVIOR IN LIDAR POINT CLOUDS OF URBAN ENVIRONMENTS. *Int. Arch. Photogramm. Remote Sens. Spat. Inf. Sci. XLII-1-W1, 543–550.* doi.org/10.5194/isprs-archives-XLII-1-W1-543-2017

Schauer, J., Nüchter, A., 2018. The Peopleremover—Removing Dynamic Objects From 3-D Point Cloud Data by Traversing a Voxel Occupancy Grid. *IEEE Robot. Autom. Lett.* 3, 1679–1686. doi.org/10.1109/LRA.2018.2801797

Shannon, C.E., 1949. Communication in the Presence of Noise. In: *IRE* 37, 10–21. doi.org/10.1109/JRPROC.1949.232969

Szutor, P., Zichar, M., 2023. Fast Radius Outlier Filter Variant for Large Point Clouds. *Data* 8, 149. doi.org/10.3390/data8100149

Tabernig, R., Albert, W., Weiser, H., Höfle, B., 2025a. A hierarchical approach for near real-time 3D surface change analysis of permanent laser scanning point clouds. In: *6th Joint International Symposium on Deformation Monitoring (JISDM)*. doi.org/10.5445/IR/1000180377

Tabernig, R., Albert, W., Weiser, H., Fritzmann, P., Anders, K., Rutzinger, M., Höfle, B., 2025b. Temporal aggregation of point clouds improves permanent laser scanning of landslides in forested areas. *Sci. Remote Sens*. 12, 100254. doi.org/10.1016/j.srs.2025.100254

Winiwarter, L., Anders, K., Schröder, D., Höfle, B., 2022. Full four-dimensional change analysis of topographic point cloud time series using Kalman filtering. *Earth Surf. Dyn*. 593–613. doi.org/10.5194/esurf-11-593-2023

Wittke, S., Campos, M., Ruoppa, L., Echriti, R., Wang, Y., Gołoś, A., Kukko, A., Hyyppä, J., Puttonen, E., 2024. LiPheStream - A 18-month high spatiotemporal resolution point cloud time series of Boreal trees from Finland. *Sci. Data* 11, 1281. doi.org/10.1038/s41597-024-04143-w

Yang, Y., Holst, C., 2025. How to Find Geometric Changes in Laser Scanning Point Clouds? A Perspective on Correspondence Definitions. *ISPRS Ann. Photogramm. Remote Sens. Spat. Inf. Sci. X-G-2025*, 1003–1010. doi.org/10.5194/isprs-annals-X-G-2025-1003-2025